

Detecting spatial clusters on functional data: a parametric scan statistic approach

Camille Frévent¹, Mohamed-Salem Ahmed¹, Matthieu Marbac², and Michaël Genin^{*,1}

¹Univ. Lille, CHU Lille, ULR 2694 - METRICS: Évaluation des technologies de santé et des pratiques médicales, F-59000 Lille, France.

²Univ. Rennes, Ensai, CNRS, CREST - UMR 9194, F-35000 Rennes, France

Abstract

This paper proposes a parametric scan statistic for detecting clusters of functional data indexed in space. The proposed method is based on an adaptation of a functional ANOVA. In a simulation study, it presents better performances than the nonparametric functional scan statistic for normal data and good performances also on quasi-normal distributions. The proposed method allows to detect smaller spatial clusters than the nonparametric one. It shows also better performances than the parametric univariate spatial scan statistic applied on the average over time. The parametric scan statistic for functional data was then applied on the search of spatial clusters of abnormal unemployment rates in France, considering the period from 1998 to 2013 divided in quarters.

Keywords: Spatial scan statistics, cluster detection, functional data

1 Introduction

Spatial cluster detection has been studied for many years to develop new tools to detect aggregation of spatial sites which behave "differently" from others. Three general categories of tests for cluster detection can be distinguished: (i) the tests for global clustering aim at evaluating if some spatial observations tend to aggregate without locating the spatial clusters, (ii) the focused cluster tests search the presence of a cluster around a fixed focus, thus they require prior knowledge since a focus determined on the data generates a pre-selection bias, and (iii) the non-focused cluster detection tests aim at detecting statistically significant spatial clusters without any *a priori* information about the localisation of the clusters. In this latter category, the spatial scan statistics are well-known methods that were applied in many applied research fields such as epidemiology (Kulldorff (1999), Luquero et al. (2011), Genin et al. (2020)), environmental sciences (Chong et al. (2013), Duncan et al. (2016)), geology (Gao et al. (2014)).

The scan statistics were first introduced in the unidimensional case by Naus (1965b) and then in the multidimensional case by Naus (1965a). The spatial scan statistics can be viewed as an extension of bidimensional scan statistics to spatial data. This extension was initially proposed by Kulldorff and Nagarwalla (1995) and Kulldorff (1997) in the cases of Bernoulli and Poisson models. They present a method based on the likelihood ratio and Monte-Carlo testing to detect significant clusters of various sizes and shapes. Following on from Kulldorff's initial work, several researchers have adapted spatial scan statistics to other spatial data distributions, such as ordinal (Jung et al. (2007)), normal (Kulldorff et al. (2009)), exponential (Huang et al. (2007)), and Weibull models (Bhatt and Tiwari

*Corresponding author: michael.genin@univ-lille.fr

(2014)). [Kulldorff et al. \(2007\)](#) developed a parametric scan statistic in the case of multivariate spatial data. However this method based on a combination of independent univariate scan statistics fails to take into account the correlations between the variables. This issue was circumvented by [Cucala et al. \(2017\)](#) who proposed a spatial scan statistic using a likelihood ratio based on a multivariate normal probability model which takes into account the correlations between the variables.

Nowadays, with sensor expansion and the increasing storage capacity, more and more data are measured in quasi-continuous time. This led to the introduction of functional data analysis (FDA) by [Ramsay and Silverman \(2005a\)](#). A considerable work has been done on the representation, exploration and modeling of functional data since with the adaptation of classical statistical methods to the functional framework such as principal component analysis ([Boente and Fraiman \(2000\)](#), [Berrendero et al. \(2011\)](#)) or regression ([Cuevas et al. \(2002\)](#), [Ferraty and Vieu \(2002\)](#), [Chiou and Müller \(2007\)](#)).

Nonparametric methods have also been developed for functional data, and an overview is available in [Ferraty and Vieu \(2006\)](#). FDA is thus an active research topic with potential applications in a large number of fields.

In the field of spatial scan statistics, a "naive" univariate approach based on the averaged data in each spatial location during the studied period would lead to a huge loss of information. A multivariate method, considering each time of observation as a variable would face with high dimensionality and high correlation issues. Recently, [Smida et al. \(2020\)](#) proposed a nonparametric approach based on a functional Wilcoxon-Mann-Whitney test. To our knowledge, no parametric scan statistic for functional data has been proposed. However since an ANOVA test for functional data was proposed by [Cuevas et al. \(2004\)](#), a scan procedure based on this test should be considered.

In this paper a parametric spatial scan statistic for functional data, based on a functional ANOVA is proposed. Section 2 presents the methodology of the parametric spatial scan statistic. The performances of this new approach are then evaluated through a simulation study and compared to the one proposed by [Smida et al. \(2020\)](#) in Section 3. The method is applied on a real dataset in Section 4. Finally the results are discussed in Section 5.

2 A parametric spatial scan statistic for univariate functional data

2.1 General principle

Let s_1, \dots, s_n be n non-overlapping locations of an observation domain $S \subset \mathbb{R}^2$ and X_1, \dots, X_n be the observations of X in s_1, \dots, s_n . Hereafter, all observations are considered to be independent, this is a classical assumption in scan statistics. The aim of spatial scan statistics is to detect spatial clusters and to test their statistical significance. It is used as a test statistic for testing a null hypothesis \mathcal{H}_0 : absence of a cluster against a composite alternative hypothesis \mathcal{H}_1 : presence of at least one cluster $w \subset S$ presenting abnormal values of X .

When $X \in \mathbb{R}$, parametric univariate scan statistics aim at detecting aggregates of locations in which the mean of X is higher or lower than the mean of X outside using often likelihood ratios ([Kulldorff et al. \(2009\)](#)). In that case a cluster w can be defined by $\mathbb{E}[X_i | s_i \in w] = \mathbb{E}[X_i | s_i \notin w] + \Delta$ where $\Delta \neq 0$. In the same way, in the multivariate case ($X \in \mathbb{R}^d$, $d \geq 2$), parametric spatial scan statistics also use likelihood ratios ([Kulldorff et al. \(2007\)](#), [Cucala et al. \(2017\)](#)) to detect aggregates of locations in which the values of the random vector X are abnormally high or low. Then a cluster w in this framework can be characterized by $\mathbb{E}[X_i | s_i \in w] = \mathbb{E}[X_i | s_i \notin w] + \Delta$ where $\Delta = (\Delta_1, \dots, \Delta_d)^\top \neq 0$, and for all $i \in \llbracket 1; d \rrbracket$, $\Delta_i \geq 0$ or for all $i \in \llbracket 1; d \rrbracket$, $\Delta_i \leq 0$.

In the functional framework, $\{X(t), t \in \mathcal{T}\}$ is a real-valued stochastic process where \mathcal{T} is an interval of \mathbb{R} . Two types of clusters can be distinguished for functional data: following Dai & Genton's work ([Dai and Genton \(2019\)](#)) that identifies magnitude outlyingness and shape outlyingness, *magnitude clusters* and *shape clusters* can be defined. Thus analogously to the univariate and multivariate definitions, a *magnitude cluster* w can be defined as follows:

$$\forall t \in \mathcal{T}, \mathbb{E}[X_i(t) | s_i \in w] = \mathbb{E}[X_i(t) | s_i \notin w] + \Delta(t), \quad (1)$$

where Δ is of constant sign, and non-zero over at least one sub-interval of \mathcal{T} . In the same way, a *shape cluster* w can be defined as follows:

$$\forall t \in \mathcal{T}, \mathbb{E}[X_i(t) \mid s_i \in w] = \mathbb{E}[X_i(t) \mid s_i \notin w] + \Delta(t) \quad (2)$$

where Δ is not constant almost everywhere.

Since the article of [Cressie \(1977\)](#), the spatial scan statistic can be defined as the maximum of a concentration index over a set of potential clusters \mathcal{W} . It thus depends on the choice of the concentration index and of \mathcal{W} . In the following, without loss of generality, \mathcal{W} is composed of circular clusters as introduced by [Kulldorff \(1997\)](#): denoting by $|w|$ the number of sites in w ,

$$\mathcal{W} = \{w_{i,j} \mid 1 \leq |w_{i,j}| \leq \frac{n}{2}, 1 \leq i, j \leq n\}, \quad (3)$$

where $w_{i,j}$ is the disc centered on s_i and passing through s_j : a cluster cannot cover more than 50 % of the studied region. It should be noted that many other shapes have been suggested such as elliptical clusters ([Kulldorff et al. \(2006\)](#)), rectangular clusters ([Chen and Glaz \(2009\)](#)) or graph-based clusters ([Cucala et al. \(2013\)](#)).

The next subsection will define a concentration index for functional univariate data.

2.2 Test statistic

In the same manner as in the univariate and multivariate frameworks, the parametric concentration index defined here will compare the mean functions between the potential clusters and the outside.

From now the process X is supposed to take values in the space $L^2(\mathcal{T}, \mathbb{R})$ of real valued square-integrable functions on \mathcal{T} , and the observations X_1, \dots, X_n of X in s_1, \dots, s_n are supposed to be independant.

[Cuevas et al. \(2004\)](#) and [Górecki and Smaga \(2015\)](#) proposed an adaptation of the classical ANOVA F-statistic for L^2 processes. Without loss of generality, considering two independent samples of trajectories drawn from two L^2 processes X_{g_1} and X_{g_2} in two groups g_1 and g_2 , it compares the mean functions μ_{g_1} and μ_{g_2} where $\mu_{g_i}(t) = \mathbb{E}[X_{g_i}(t)]$, $i = 1, 2$.

Thus, in the context of cluster detection, the null hypothesis \mathcal{H}_0 (absence of cluster) can be defined as follows: $\mathcal{H}_0 : \forall w \in \mathcal{W}, \mu_w = \mu_{w^c} = \mu_S$, where μ_w , μ_{w^c} and μ_S stand for the mean functions in w , outside w and over S , respectively. The alternative hypothesis $H_1^{(w)}$ associated to a potential cluster w can be defined as follows: $H_1^{(w)} : \mu_w \neq \mu_{w^c}$. Then the functional ANOVA can be used to compare the mean function in w with the mean function in w^c by using the following statistic:

$$F_n^{(w)} = \frac{|w| \|\bar{X}_w - \bar{X}\|_2^2 + |w^c| \|\bar{X}_{w^c} - \bar{X}\|_2^2}{\frac{1}{n-2} \left[\sum_{j, s_j \in w} \|X_j - \bar{X}_w\|_2^2 + \sum_{j, s_j \in w^c} \|X_j - \bar{X}_{w^c}\|_2^2 \right]}, \quad (4)$$

where $\bar{X}_g(t) = \frac{1}{|g|} \sum_{i, s_i \in g} X_i(t)$ are empirical estimators of μ_g ($g \in \{w, w^c\}$), $\bar{X}(t) = \frac{1}{n} \sum_{i=1}^n X_i(t)$ is the

empirical estimator of μ_S and $\|x\|_2^2 = \int_{\mathcal{T}} x^2(t) dt$.

Thus, $F_n^{(w)}$ can be considered as a concentration index and maximized over the set of potential clusters \mathcal{W} , yielding to the following definition of the parametric functional spatial scan statistic (PFSS):

$$\Lambda_{\text{PFSS}} = \max_{w \in \mathcal{W}} F_n^{(w)}, \quad (5)$$

and the potential cluster for which this maximum is obtained, namely, the most likely cluster (MLC) is

$$\text{MLC} = \arg \max_{w \in \mathcal{W}} F_n^{(w)}. \quad (6)$$

2.3 Computing the significance of the MLC

Once the most likely cluster has been detected, its statistical significance must be evaluated. However, due to the overlapping nature of \mathcal{W} , the distribution of Λ_{PFSS} has no closed form under \mathcal{H}_0 . Since no distribution for the observations has been assumed, the solution chosen by [Kulldorff \(1997\)](#) that consists in simulating datasets under \mathcal{H}_0 is not applicable. Then the chosen strategy was to create a large set of random datasets by randomly permuting the observations X_i in the spatial locations. This technique called "random labelling" was already used in spatial scan statistics ([Kulldorff et al. \(2009\)](#), [Cucala et al. \(2017\)](#), [Cucala et al. \(2019\)](#)).

Let M denote the number of random permutations of the original dataset and $\Lambda_{\text{PFSS}}^{(1)}, \dots, \Lambda_{\text{PFSS}}^{(M)}$ be the observed scan statistics on the simulated datasets. According to [Dwass \(1957\)](#) the p-value for $\mathcal{S}_{\mathcal{W}}$ observed on the real data is estimated by

$$\hat{p} = \frac{1 + \sum_{m=1}^M \mathbb{1}_{\Lambda_{\text{PFSS}}^{(m)} \geq \Lambda_{\text{PFSS}}}}{M + 1}. \quad (7)$$

Finally, the MLC is considered as statistically significant if the associated \hat{p} is less than the type I error.

3 A simulation study

We performed a simulation study in order to compare the performances of the parametric functional spatial scan statistic (PFSS) Λ_{PFSS} , with (i) the nonparametric functional spatial scan statistic (NPFSS) Λ_{NPFSS} proposed by [Smida et al. \(2020\)](#), (ii) the parametric univariate spatial scan statistic (PUSS) Λ_{PUSS} proposed by [Kulldorff et al. \(2009\)](#) and (iii) the nonparametric univariate spatial scan statistic (NPUSS) Λ_{NPUSS} introduced by [Jung and Cho \(2015\)](#). For these last two methods, the average over the time of the observations in each site was considered.

It should be noted that the design of this simulation study is deliberately close to that proposed in the article of [Smida et al. \(2020\)](#) in order to consider different data distributions.

As stated by [Smida et al. \(2020\)](#), the NPFSS appears to be very time-consuming since for each potential cluster w it needs to sum $|w|(n - |w|)$ terms. Although the authors proposed a first computation improvement, the number of calculations remains still elevated. Thus, in the context of this simulation study, we proposed an improvement of the NPFSS computation that significantly reduces the computing time. Optimization details and examples of computation time are provided in the Appendix, Section B.

3.1 Design of simulation study

Artificial datasets were generated by using the geographic locations of the 94 French *départements* (administrative areas) as shown in Figure 1. The location of each *département* was defined by its administrative center. A true cluster w composed of eight *départements* was defined in the Parisian area and simulated for each artificial dataset (see the red area in Figure 1).

3.1.1 Generation of the artificial datasets

The X_i are generated using the Karhunen–Loève decomposition:

$$\text{for each } i \in \llbracket 1; 94 \rrbracket, X_i(t) = \sum_{k=1}^{100} Z_k \phi_k(t) + \Delta(t) \mathbb{1}_{s_i \in w}, \quad t \in [0; 1].$$

$\{\phi_k(t) = \sqrt{2} \sin[(k - 0.5)\pi t]\}$ is an orthonormal basis of $L^2([0; 1], \mathbb{R})$. The Z_k are pairwise uncorrelated random variables and the functions X_i are measured at 101 equally spaced times on $[0; 1]$.

Giving $\sigma_k = [(k - 0.5)\pi]^{-1}$, three distributions for the X_i were considered: (i) a Gaussian process: $\frac{Z_k}{\sigma_k}$ have a $\mathcal{N}(0, 1)$ distribution, (ii) a centered Student process with three degrees of freedom ($t(3)$) and



Figure 1: The 94 French *départements* and the true cluster (in red) simulated for each artificial dataset.

(iii) a centered Student process with five degrees of freedom ($t(5)$): $\frac{Z_k}{\sigma_k} = U_k \left(\frac{V_d}{d}\right)^{-0.5}$ for $d = 3$ and $d = 5$, where the U_k are independent $\mathcal{N}(0, 1)$ variables, and V_d is independent of the U_k and has a chi-square distribution with d degrees of freedom.

Two types of clusters were simulated with intensity controlled by some parameter $\alpha > 0$. The two chosen shifts Δ vary over time and are positive and non-zero (except possibly in $t = 0$ or $t = 1$): $\Delta_1(t) = \alpha t$ and $\Delta_2(t) = \alpha t(1 - t)$. Thus they correspond to both magnitude and shape clusters. Different values of the true cluster intensity were considered for each Δ . Since Δ_2 takes lower values over the time than Δ_1 for the same value of α , bigger cluster intensity values are taken for Δ_2 . Remark that $\alpha = 0$ was also tested in order to evaluate the maintain of the nominal type I error. Thus for Δ_1 , $\alpha \in \{0; 0.75; 1.5; 2.25; 3\}$ and for Δ_2 , $\alpha \in \{0; 2; 4; 6; 8\}$. An example of the data for the Gaussian process is presented in the Appendix (Figure 5).

3.1.2 Comparison of the methods

For each type of process, each type of Δ and each value of α , 1000 artificial datasets were simulated. The p-value associated to each MLC was estimated by generating 999 random permutations of the data. A type I error of 5 % was considered for the rejection of \mathcal{H}_0 . The performances of the four methods were compared with regard to four criteria: the power, the true positive rate, the false positive rate and the positive predicted value.

The power was estimated by the proportion of simulations yielding to the rejection of \mathcal{H}_0 according to the type I error. Among the simulated datasets yielding to rejection of \mathcal{H}_0 , the true positive rate is the average proportion of sites correctly detected among the sites in w , the false positive rate is the average proportion of sites in w^c that were included in the detected cluster and the positive predictive value corresponds to the average proportion of sites in w among the detected cluster.

3.1.3 Results of the simulation study

The results of the simulation are presented in Figure 2. For $\alpha = 0$, the different methods seem to maintain the correct type I error of 0.05 regardless of the type of process and Δ (see power curves in Figure 2). As expected, the higher is α the better are the performances, for every method.

For the Gaussian process, the nonparametric and the parametric functional methods show better results than the corresponding univariate ones. The power curves are close between the different approaches. However for $\Delta = \Delta_1$, the differences between the functional methods and the univariate ones are more marked with a higher power for the functional ones compared to the corresponding univariate ones. Moreover, for $\Delta = \Delta_1$, the PFSS shows higher powers than the NPFSS, contrary to the case $\Delta = \Delta_2$ for which the power curves of all methods except the NPUSS are similar. The NPFSS presents higher true positive rates than the PFSS. However the latter gives lower false positive rates: the NPFSS approaches seems to detect bigger clusters than the PFSS. Moreover the univariate methods always present higher false positive rates and often lower true positive rates than the corresponding functional method. Finally the parametric methods present higher positive predictive values and the functional methods often present higher positive predictive values than the corresponding univariate method.

For the Student process $t(3)$, the nonparametric methods show higher powers than the parametric ones. As in the case of the Gaussian process, they tend to exhibit larger clusters than the parametric methods since the true positive rates and the false positive rates are higher. As expected, the performances of the parametric methods decreased since the data distribution deviates significantly from normality. The positive predictive value is very close for all methods.

For the Student process $t(5)$, the powers of the PFSS and the PUSS are close to the powers of the nonparametric methods. The true positive rates increase and the false positive rates remain very low. Finally the parametric methods present again higher positive predictive values than the nonparametric ones and the functional methods often show higher positive predictive values than the corresponding univariate ones.

4 Application on real data

4.1 Unemployment rates in France

The data considered is unemployment rates provided by the *Institut National de la Statistique et des Etudes Economiques* (INSEE). It consists in the rates of unemployment in France for each quarter between 1998 and 2013 (64 values) and each of the 94 French *départements* located by their administrative center. The unemployment rate curves (from 1998 to 2013) in each *département* are presented in Figure 3 (left panel). The spatial distribution of the mean unemployment rates over the studied time period is presented in Figure 3 (right panel).

The map in Figure 3 shows a spatial heterogeneity of the average unemployment rates. High unemployment rates tend to aggregate both in the northern and southeastern France. Moreover, the unemployment rates curves show a marked temporal variability during the period from 1998 to 2013. these two observations strongly suggest the use of functional spatial scan statistics in order to objectify the presence of spatial clusters of unemployment rates.

4.2 Spatial clusters detection

In order to detect spatial clusters of low or elevated unemployment rates, the PFSS and the NPFSS were considered.

The most likely cluster is considered together with the secondary clusters that had a high value of the concentration index ($F_n^{(w)}$ for PFSS, and $U(w)$ for NPFSS (see Smida et al. (2020) for details)) and did not cover the MLC (Kulldorff (1997)). For both methods, we considered a circular variable scanning window of maximum size such that a cluster never contains more than 50 % of total number of *départements*. The statistical significance of both MLC and secondary clusters were evaluated through 999 Monte-Carlo permutations. A spatial cluster was considered as statistically significant at the type I error of 0.05.

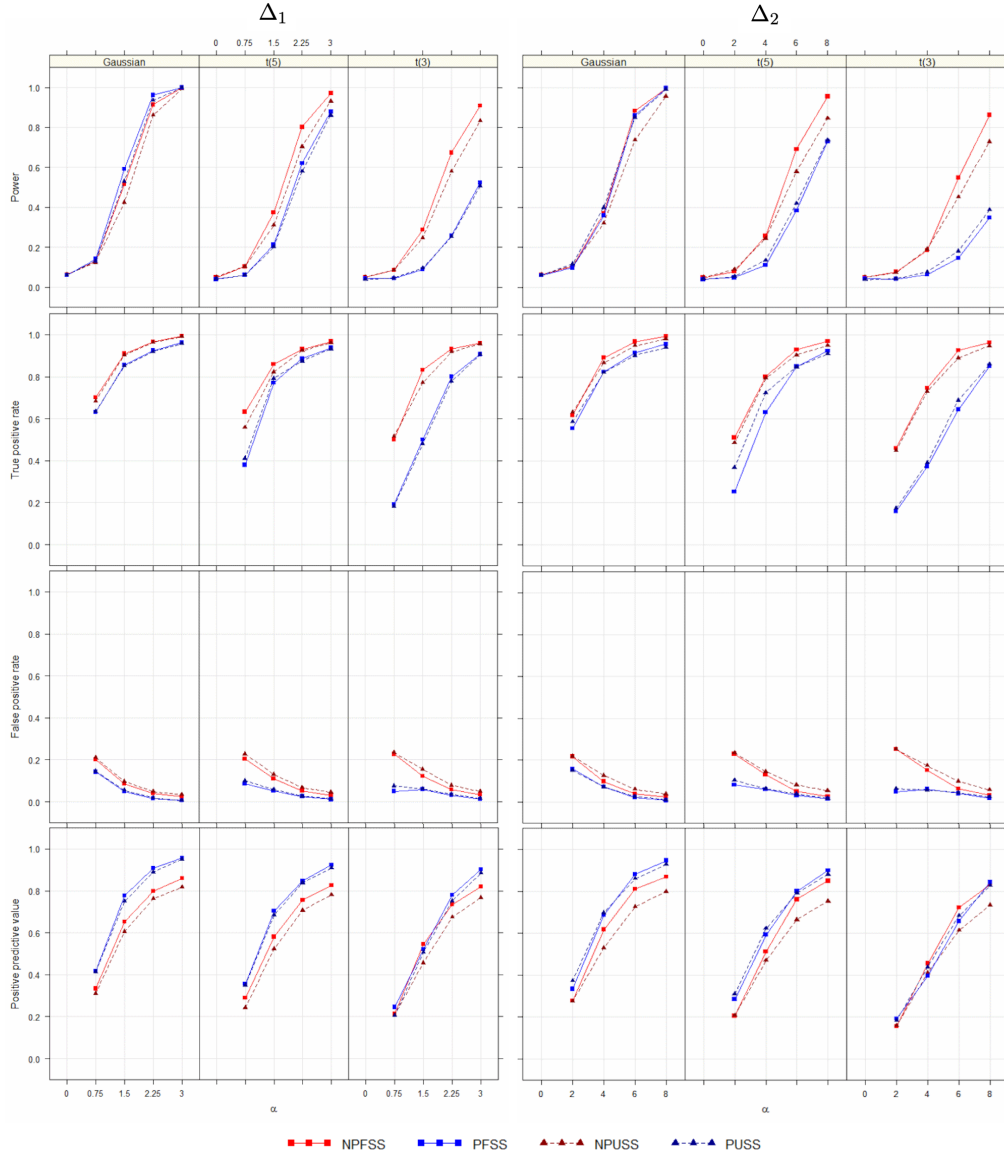


Figure 2: Simulation study: comparison of the NPUSS, the PUSS, the NPFSS and the PFSS methods for two types of shift Δ : $\Delta_1(t) = \alpha t$ (left panel) and $\Delta_2(t) = \alpha t(1 - t)$ (right panel). For each method, the power curves, the true-positive and false-positive rates and the positive predictive values for the detection of the true cluster as most likely cluster are shown. The quantity α refers to the parameter controlling the cluster intensity.

4.3 Results

Both methods detected two significant spatial clusters that are presented in Figure 4 and described in Table 1.

The PFSS identified two significant spatial clusters of elevated unemployment rates: the MLC (7 *départements*, $\hat{p} = 0.011$) located in southeastern France and the secondary cluster (9 *départements*, $\hat{p} = 0.039$) located in northern France. These clusters are homogeneous since they contain only curves that are above the average unemployment rate curve (excepting two *départements* curves in the secondary cluster that are below the average curve at the beginning of the period).

The NPFSS identified a significant large MLC ($\hat{p} = 0.013$) of low unemployment rates located in the center of France and containing 40 *départements*. This MLC shows a high heterogeneity of unemployment rates curves, including some *départements* with a unemployment rate over the average unemployment rate (see unemployment rate curves in Figure 4). The secondary cluster detected by this method (9 *départements*, $\hat{p} = 0.039$) is exactly the same as the one detected by the PFSS.

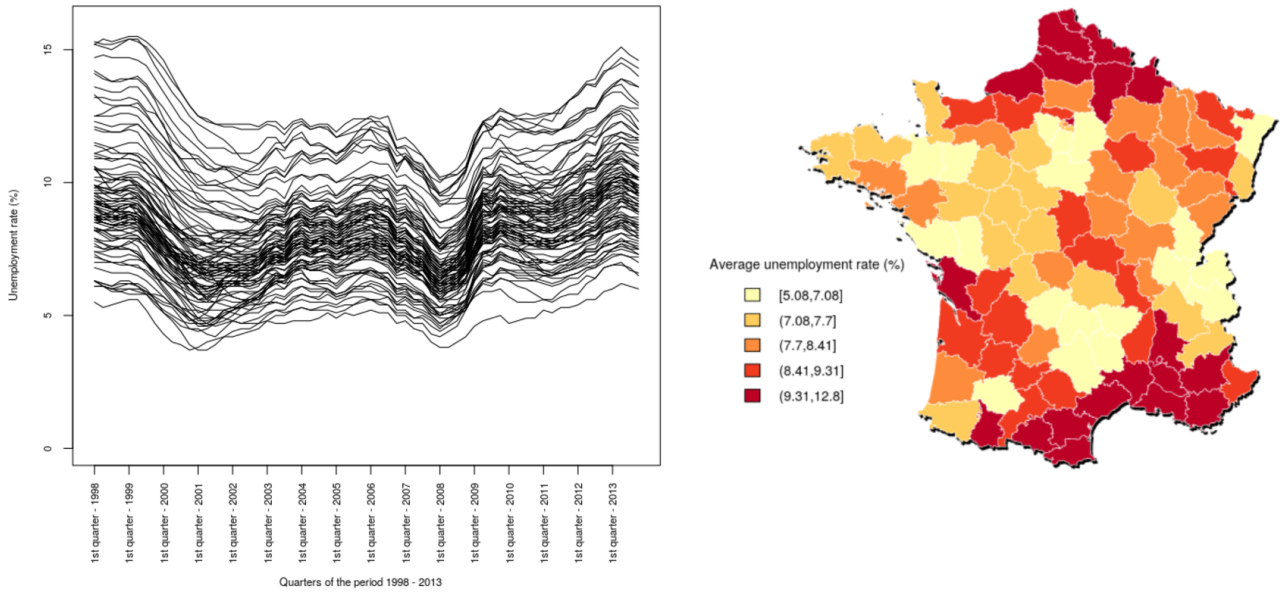


Figure 3: Unemployment rate curves (from 1998 to 2013) in each of the 94 French *départements* (left panel), and spatial distribution of the mean unemployment rates over period from 1998 to 2013 (right panel).

Table 1: Statistically significant spatial clusters of higher or lower unemployment rates detected for the parametric (PFSS) and the nonparametric (NPFSS) functional methods

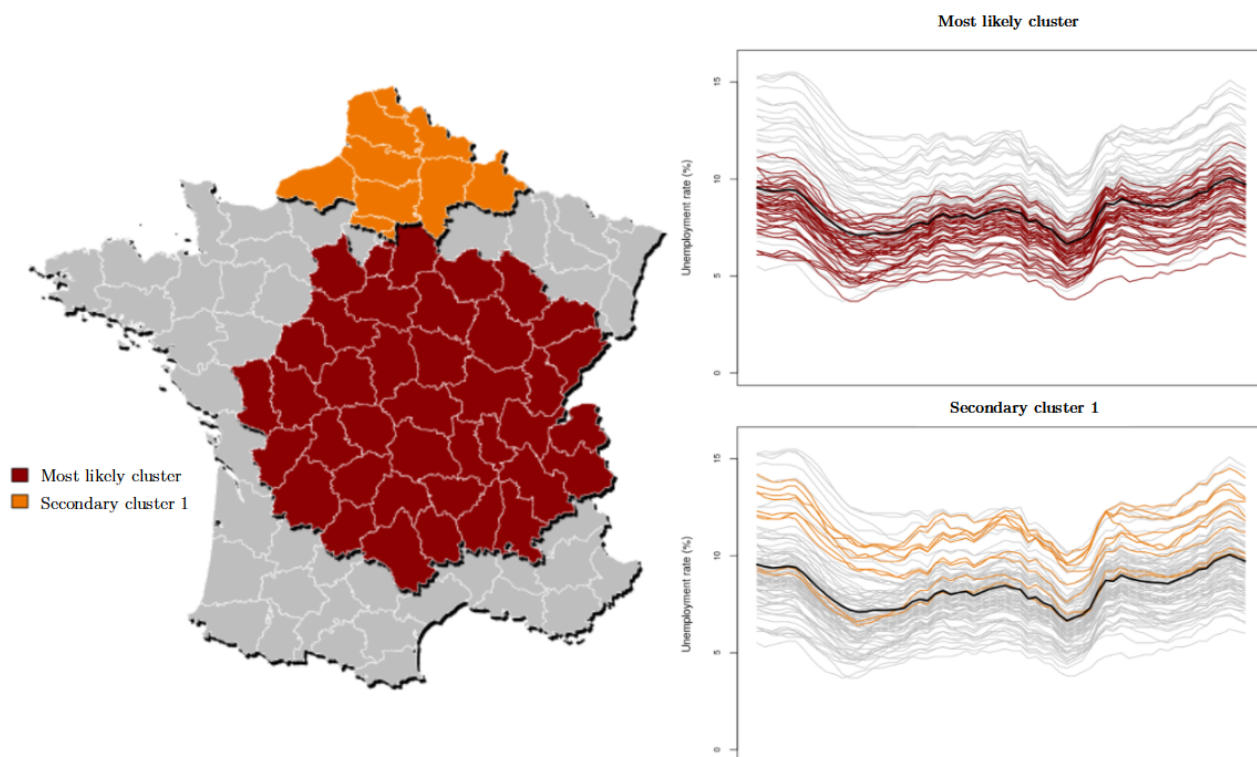
	Cluster	# <i>départements</i>	p-value	Mean (sd) value inside	Mean (sd) value outside
NPFSS	1	40	0.013	7.47 (1.38)	8.91 (2.06)
	2	9	0.039	10.52 (1.69)	8.06 (1.81)
PFSS	1	7	0.011	11.03 (1.79)	8.08 (1.77)
	2	9	0.039	10.52 (1.69)	8.06 (1.81)

5 Discussion

Here, we developed a parametric functional spatial scan statistics (PFSS) aiming at detecting clusters of functional data indexed in space. The PFSS is based on the adaptation of the ANOVA F-Statistic, initially proposed by Cuevas et al. (2004), as a concentration index for spatial scan statistic. Compared to univariate spatial scan statistic approaches, our method appears to be more relevant in case of functional spatial data since the former involve summarizing the data by averaging them over the time period which can lead to an important loss of information. Compared to the multivariate spatial scan statistic approaches, our method appears to be still more relevant because it faces both the problem of high dimensionality and high correlation between time measurement.

In a simulation study, the method was compared with the NPFSS proposed by Smida et al. (2020) and with nonparametric (NPUSS) and parametric (PUSS) univariate methods considering the average of the variable of interest over the time period. The simulation study highlighted that globally, the functional methods showed better performances than the corresponding univariate ones. It sounds logical since the univariate methods take the mean over the time period of the variable which leads to a loss of information in comparison with functional methods. In case of normal data the PFSS presented better performances than the NPFSS. They were close in terms of power, however the NPFSS tended to detect larger clusters. When the data were strongly non-normal, the performances of the PFSS decreased. In that case the use of the NPFSS seemed to be more appropriate. However, when the data were close to the normality the power of the PFSS was close to the one of the NPFSS and the

Clusters for the NPFSS



Clusters for the PFSS

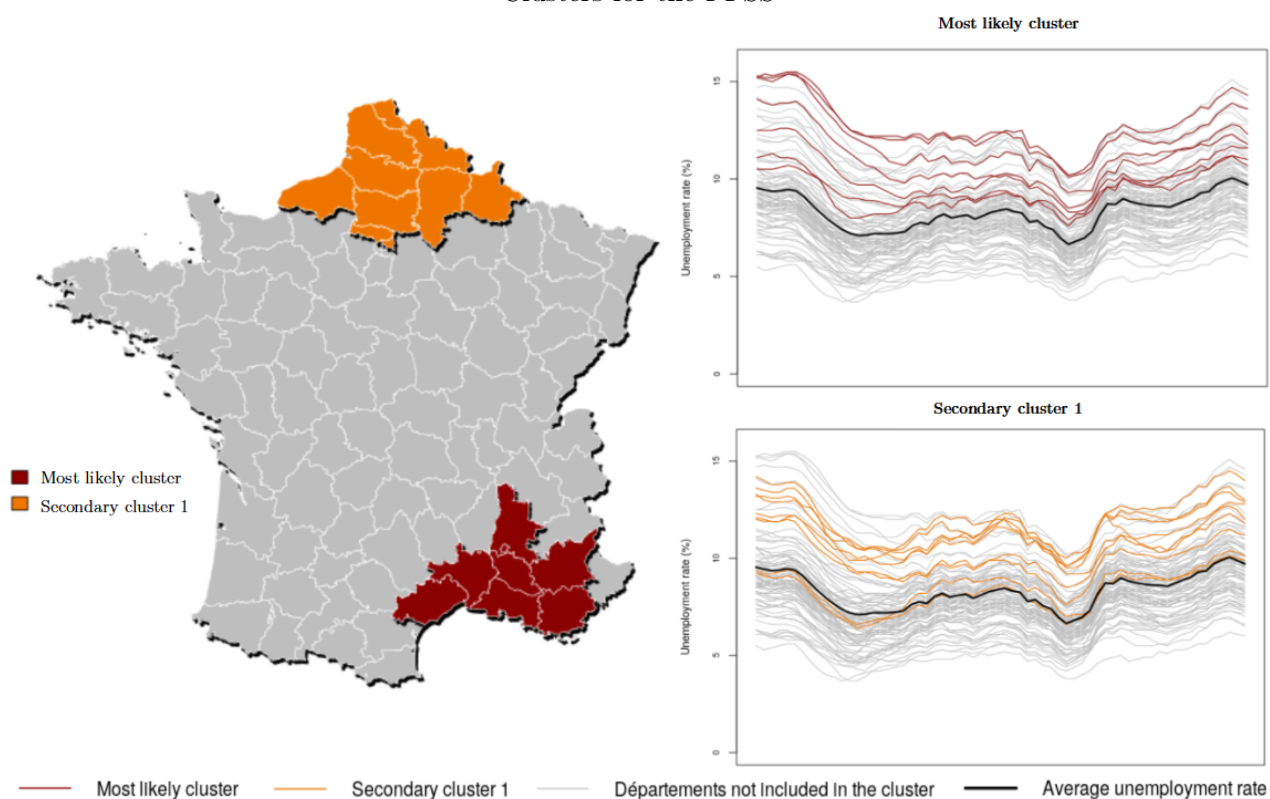


Figure 4: Significant spatial clusters of high or low unemployment rates detected by the NPFSS (top panel) and the PFSS (bottom panel). Spatial clusters in red are the most likely cluster for each method and the ones in orange represent the secondary clusters. For each cluster the unemployment rate curves (from 1998 to 2013) in each *département* are presented with colored lines. The black curve is the average unemployment rate in France.

PFSS presented the advantage to detect smaller clusters which may be more relevant in numerous applications. Moreover the positive predictive value of the PFSS was almost always better than the NPFSS, thus improving the confidence in the clusters detected by this method.

The same conclusions could be established in the application on real data. The PFSS and the NPFSS were applied to detect clusters of abnormal values of unemployment rates in the 94 French *départements*. The NPFSS detected a most likely cluster composed of 40 *départements* in the center of France. Although it was a cluster of low unemployment rates, it contained many *départements* with high unemployment rates curves, which makes it non-relevant, all the more so as the identified cluster covered approximately half of France. In comparison, the most likely cluster for the PFSS was only composed of 7 *départements* in the southeastern France. It contained only *départements* with high unemployment rates curves. Both approaches detect the same secondary cluster of high unemployment rates in the northern France.

It should be noticed that the PFSS only deals with round-shaped clusters. In the application to the unemployment data, an elongated aggregation of *départements* of high unemployment rates was observed in southern France, yielding to the fact that other cluster shape could be considered in the analysis. The PFSS can easily be adapted to other cluster shape such as elliptic clusters (Kulldorff et al. (2006)) or graph-based clusters (Cucala et al. (2013)).

Remark that, in both the simulation study and the application to real data, the observations times were identical for every spatial locations. Although it is an ideal situation when dealing with functional data, it is relatively rare in numerous real data. However the method could be still applied in the case of different observation times in the spatial location by applying well-know smoothing methods on the raw data such as projection into a B-spline basis (for details, see Ramsay and Silverman (2005b)).

The PFSS is derived from the ANOVA test for functional data introduced by Cuevas et al. (2004). More recently, Srivastava et al. (2013) proposed another two-sample test statistic for functional data but it appears to be very time consuming and we did not consider it for the present spatial scan statistic. Actually, the concentration index is firstly calculated for each potential cluster in the detection step of the MLC, and, secondly, when computing the statistical significance of the latter, the detection step is performed for each permutation of the data. Thus, we considered the Cuevas' approach because it yields to a reasonable computing time for the spatial scan statistic.

The PFSS is designed for dealing with univariate functional data but the multivariate functional case should also be investigated. As an example, one may consider the data from sensors located in different geographical locations, each sensor simultaneously measuring several air pollutants over time. In this case, the detection of significant spatial clusters can help experts to identify environmental black-spots. The PFSS could be extended to the multivariate functional framework by adapting the multivariate ANOVA for functional data proposed by Górecki and Smaga (2017). It should be noticed that the functional Wilcoxon-Mann-Whitney test proposed by Chakraborty and Chaudhuri (2014) can also be adapted to multivariate functional data by considering a suitable scalar product for such processes for calculating the sign function.

References

- Berrendero, J., A. Justel, and M. Svarc (2011). Principal components for multivariate functional data. Computational Statistics & Data Analysis 55, 2619–2634.
- Bhatt, V. and N. Tiwari (2014). A spatial scan statistic for survival data based on weibull distribution. Statistics in medicine 33(11), 1867–1876.
- Boente, G. and R. Fraiman (2000). Kernel-based functional principal components. Statistics & Probability Letters 48, 335–345.
- Bosq, D. (2000). Linear Processes in Function Spaces, Volume 149 of Lecture Notes in Statistics. Springer.
- Chakraborty, A. and P. Chaudhuri (2014). A wilcoxon-mann-whitney type test for infinite dimensional data. Biometrika 102.
- Chen, J. and J. Glaz (2009). Scan Statistics, Chapter Approximations for Two-Dimensional Variable Window Scan Statistics, pp. 109 – 128. Birkhäuser Boston.
- Chiou, J.-M. and H.-G. Müller (2007, 06). Diagnostics for functional regression via residual processes. Computational Statistics & Data Analysis 15, 4849–4863.
- Chong, S., M. Nelson, R. Byun, L. Harris, J. Eastwood, and B. Jalaludin (2013). Geospatial analyses to identify clusters of adverse antenatal factors for targeted interventions. International journal of health geographics 12(46).
- Cressie, N. (1977). On some properties of the scan statistic on the circle and the line. Journal of Applied Probability 14, 272–283.
- Cucala, L. (2014). A distribution-free spatial scan statistic for marked point processes. Spatial Statistics 10, 117–125.
- Cucala, L. (2016). A mann-whitney scan statistic for continuous data. Communications in Statistics - Theory and Methods 45(2), 321 – 329.
- Cucala, L. (2018). Variable window scan statistics: Alternatives to generalized likelihood ratio tests. In Handbook of scan statistics. Springer.
- Cucala, L., C. Demattei, P. Lopes, and A. Ribeiro (2013). A spatial scan statistic for case event data based on connected components. Computational Statistics 28, 357–369.
- Cucala, L., M. Genin, C. Lanier, and F. Occelli (2017). A multivariate gaussian scan statistic for spatial data. Spatial Statistics 21, 66–74.
- Cucala, L., M. Genin, F. Occelli, and J. Soula (2019). A multivariate nonparametric scan statistic for spatial data. Spatial statistics 29, 1–14.
- Cuevas, A., M. Febrero-Bande, and R. Fraiman (2002). Linear functional regression: The case of fixed design and functional response. Canadian Journal of Statistics 30, 285–300.
- Cuevas, A., M. Febrero-Bande, and R. Fraiman (2004). An anova test for functional data. Computational Statistics & Data Analysis 47, 111–122.
- Dai, W. and M. G. Genton (2019). Directional outlyingness for multivariate functional data. Computational Statistics & Data Analysis 131, 50–65.
- Duncan, D., M. Rienti, M. Kulldorff, J. Aldstadt, M. Castro, R. Frounfelker, J. Williams, G. Sorensen, R. Johnson, D. Hemenway, and D. Williams (2016). Local spatial clustering in youths’ use of tobacco, alcohol, and marijuana in boston. The American journal of drug and alcohol abuse 42(4), 412–421.

- Dwass, M. (1957). Modified randomization tests for nonparametric hypotheses. Annals of Mathematical Statistics 28(1), 181–187.
- Ferraty, F. and P. Vieu (2002). Functional nonparametric model and application to spectrometric data. Computational Statistics 17, 545–564.
- Ferraty, F. and P. Vieu (2006). Nonparametric Functional Data Analysis. Springer Series in Statistics. Springer.
- Gao, J., Z. Zhang, Y. Hu, J. Bian, W. Jiang, X. Wang, L. Sun, and Q. Jiang (2014). Geographical distribution patterns of iodine in drinking-water and its associations with geological factors in shandong province, china. International journal of environmental research and public health 11(5), 5431–5444.
- Genin, M., M. Fumery, F. Occelli, G. Savoye, B. Pariente, L. Dauchet, J. Giovannelli, C. Vignal, M. Body-Malapel, H. Sarter, et al. (2020). Fine-scale geographical distribution and ecological risk factors for crohn’s disease in france (2007-2014). Alimentary Pharmacology & Therapeutics 51(1), 139–148.
- Górecki, T. and Ł. Smaga (2015). A comparison of tests for the one-way anova problem for functional data. Computational Statistics 30, 987–1010.
- Górecki, T. and Ł. Smaga (2017). Multivariate analysis of variance for functional data, journal of applied statistics. Journal of Applied Statistics 44(12), 2172–2189.
- Horváth, L. and P. Kokoszka (2012). Inference for Functional Data with Applications. Springer Series in Statistics. Springer.
- Horváth, L., P. Kokoszka, and R. Reeder (2013). Estimation of the mean of functional time series and a two sample problem. Journal of the Royal Statistical Society. Series B. 75.
- Huang, L., M. Kulldorff, and D. Gregorio (2007). A spatial scan statistic for survival data. Biometrics 63(1), 109–118.
- Jung, I. and H. J. Cho (2015). A nonparametric spatial scan statistic for continuous data. International Journal of Health Geographics 14(30).
- Jung, I., M. Kulldorff, and A. C. Klassen (2007). A spatial scan statistic for ordinal data. Statistics in medicine 26(7), 1594–1607.
- Klassen, A. C., M. Kulldorff, and F. Curriero (2005). Geographical clustering of prostate cancer grade and stage at diagnosis, before and after adjustment for risk factors. International journal of health geographics 4(1).
- Kulldorff, M. (1997). A spatial scan statistic. Communications in Statistics - Theory and Methods 26, 1481–1496.
- Kulldorff, M. (1999). Spatial Scan Statistics: Models, Calculations, and Applications, pp. 303–322.
- Kulldorff, M., R. Heffernan, J. Hartman, R. Assunção, and F. Mostashari (2005). A space–time permutation scan statistic for disease outbreak detection. PLoS Medicine 2(3).
- Kulldorff, M., L. Huang, and K. Konty (2009). A scan statistic for continuous data based on the normal probability model. Int J Health Geogr 8(58).
- Kulldorff, M., L. Huang, L. Pickle, and L. Duczmal (2006). An elliptic spatial scan statistic. Statistics in medicine 25, 3929–3943.
- Kulldorff, M., F. Mostashari, L. Duczmal, W. Yih, K. Kleinman, and R. Platt (2007). Multivariate scan statistics for disease surveillance. Statistics in medicine 26, 1824–1833.

- Kulldorff, M. and N. Nagarwalla (1995). Spatial disease clusters: Detection and inference. Statistics in Medicine 14(8), 799–810.
- Luquero, F., C. Banga, D. Remartínez, P. P. P. Urrutia, E. Baron, and R. Grais (2011). Cholera epidemic in guinea-bissau (2008) : The importance of "place". PloS one 6.
- Michelozzi, P., A. Capon, U. Kirchmayer, F. Forastiere, A. Biggeri, A. Barca, and C. Perucci (2002). Adult and childhood leukemia near a high-power radio station in rome, italy. American journal of epidemiology 155, 1096–1103.
- Naus, J. I. (1965a). Clustering of random points in two dimensions. Biometrika 52, 263–267.
- Naus, J. I. (1965b). The distribution of the size of the maximum cluster of points on a line. Journal of the American Statistical Association 60(310), 532–538.
- Openshaw, S., M. Charlton, W. Colin, and A. Craft (1987). A mark 1 geographical analysis machine for the automated analysis of point data sets. International Journal of Geographical Information Systems 1, 335–358.
- Ramsay, J. and B. Silverman (2005a). Functional Data Analysis. Springer Series in Statistics. Springer.
- Ramsay, J. and B. Silverman (2005b). Principal components analysis for functional data. Functional data analysis, 147–172.
- Smida, Z., L. Cucala, and A. Gannoun (2020). A nonparametric spatial scan statistic for functional data. hal-02908496.
- Srivastava, M. S., S. Katayama, and Y. Kano (2013). A two sample test in high dimensional data. Journal of Multivariate Analysis 114, 349–358.
- Zhang, C., H. Peng, and J.-T. Zhang (2010, 02). Two samples tests for functional data. Communications in Statistics—Theory and Methods 39, 559–578.

A Example of the data in the simulation study

The following figure illustrates an example of the data for the Gaussian process in the simulation study:

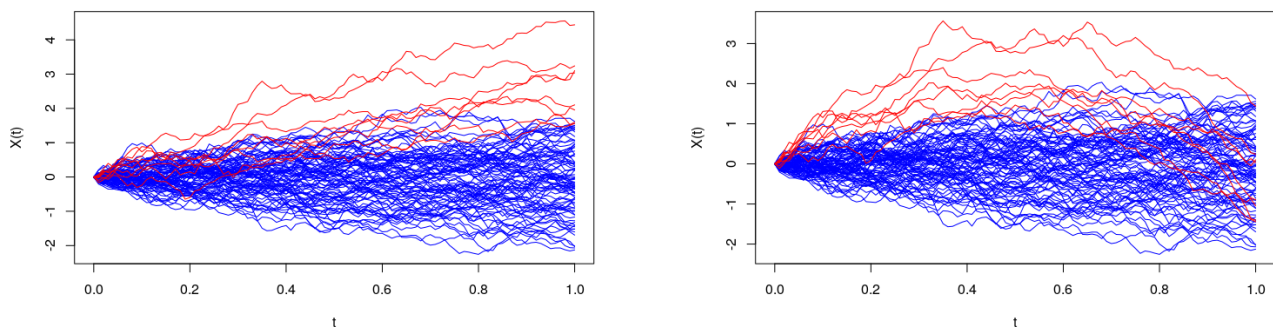


Figure 5: Simulation study: an example of the generated data for the Gaussian process with $\Delta(t) = \Delta_1(t) = 3t$ (left panel) and $\Delta(t) = \Delta_2(t) = 8t(1-t)$ (right panel). The red curves correspond to the observations in the cluster.

B Reduction of the computation time for the NPFSS

Smida et al. (2020) defined a nonparametric scan statistic for independant observations of a process in a separable Banach space χ , \mathcal{S}_W by

$$\mathcal{S}_W = \max_{w \in \mathcal{W}} \left\| \frac{1}{\sqrt{|w| |w^c| (|w| + |w^c|)}} \sum_{i, s_i \in w} \sum_{j, s_j \in w^c} \text{sign}(X_j - X_i) \right\|$$

where the sign function is the Gâteaux-derivative of the norm on χ .

Calculation of the sign function in the case of square-integrable functions

Let $X \in L^2(\mathcal{T}, \mathbb{R}) \setminus \{0\}$. In this part we will compute $\text{sign}(X)$ that is the Gâteaux-derivative of $\|X\|_2 = \sqrt{\langle X, X \rangle}$ where $\langle X, Y \rangle = \int_{\mathcal{T}} X(t)Y(t) dt$.

Let $h \in L^2(\mathcal{T}, \mathbb{R})$,

$$\begin{aligned} \lim_{v \rightarrow 0} \frac{\|X + hv\|_2 - \|X\|_2}{v} &= \lim_{v \rightarrow 0} \frac{\|X + hv\|_2^2 - \|X\|_2^2}{v(\|X + hv\|_2 + \|X\|_2)} \\ &= \lim_{v \rightarrow 0} \frac{\langle X + hv, X + hv \rangle - \langle X, X \rangle}{v(\|X + hv\|_2 + \|X\|_2)} \\ &= \lim_{v \rightarrow 0} \frac{2v\langle h, X \rangle + v^2\|h\|_2^2}{v(\|X + hv\|_2 + \|X\|_2)} \\ &= \lim_{v \rightarrow 0} \frac{2\langle h, X \rangle + v\|h\|_2^2}{\|X + hv\|_2 + \|X\|_2} \\ &= \frac{\langle h, X \rangle}{\|X\|_2}. \end{aligned}$$

Then $\text{sign}(X)(h) = \frac{\langle h, X \rangle}{\|X\|_2}$ if $X \in L^2(\mathcal{T}, \mathbb{R}) \setminus \{0\}$.

Reduction of the computation time

Let X be a stochastic process taking values in $L^2(\mathcal{T}, \mathbb{R})$, and X_1, \dots, X_n be the realizations of X in the locations s_1, \dots, s_n .

$$\text{Since the } X_i \text{ are in } L^2(\mathcal{T}, \mathbb{R}), \text{sign}(X_i) = \begin{cases} \frac{X_i}{\|X_i\|_2} & \text{if } X_i \neq 0 \\ 0 & \text{if } X_i = 0 \end{cases}.$$

Then:

$$\begin{aligned} \sum_{\substack{i=1 \\ s_i \in w}}^n \sum_{\substack{j=1 \\ s_j \in w^c}}^n \text{sign}(X_j - X_i) &= \sum_{i=1}^n \sum_{j=1}^n \text{sign}(X_j - X_i) - \sum_{\substack{i=1 \\ s_i \in w}}^n \sum_{\substack{j=1 \\ s_j \in w}}^n \text{sign}(X_j - X_i) \\ &= \sum_{i=1}^n \sum_{j=1}^n \text{sign}(X_j - X_i) - \sum_{\substack{i=2 \\ s_i \in w}}^n \sum_{\substack{j=1 \\ s_j \in w}}^n \text{sign}(X_j - X_i) - \sum_{\substack{i=1 \\ s_i \in w}}^{n-1} \sum_{\substack{j=i+1 \\ s_j \in w}}^n \text{sign}(X_j - X_i) \\ &= \sum_{i=1}^n \sum_{j=1}^n \text{sign}(X_j - X_i) - \sum_{\substack{i=2 \\ s_i \in w}}^n \sum_{\substack{j=1 \\ s_j \in w}}^n \text{sign}(X_j - X_i) + \sum_{\substack{j=1 \\ s_j \in w}}^{n-1} \sum_{\substack{i=j+1 \\ s_i \in w}}^n \text{sign}(X_j - X_i) \\ &= \sum_{i=1}^n \sum_{j=1}^n \text{sign}(X_j - X_i) - \sum_{\substack{i=2 \\ s_i \in w}}^n \sum_{\substack{j=1 \\ s_j \in w}}^n \text{sign}(X_j - X_i) + \sum_{\substack{i=2 \\ s_i \in w}}^n \sum_{\substack{j=1 \\ s_j \in w}}^{i-1} \text{sign}(X_j - X_i) \end{aligned}$$

$$= \sum_{\substack{i=1 \\ s_i \in w}}^n \sum_{j=1}^n \text{sign}(X_j - X_i)$$

Thus the matrix of signs, in which each line i corresponds to $\sum_{j=1}^n \text{sign}(X_j - X_i)$, can be computed. And

finally, to obtain $\sum_{\substack{i=1 \\ s_i \in w}}^n \sum_{\substack{j=1 \\ s_j \in w^c}}^n \text{sign}(X_j - X_i)$, it suffices to sum the rows of the matrix that correspond to the sites in w .

In order to evaluate the order of magnitude of the reduction in computing time, let consider the following example: 1000 datasets of the standard Brownian motion observed in 101 equally spaced times of $[0; 1]$ were simulated. The shift Δ was chosen such that $\Delta(t) = 2t$. The computation time of the improved method also took into account the computation time of the matrix of signs. The computation times of both methods are presented in Table 2. In this example, our method divided by approximately 100 the computing time.

Table 2: Comparison of the computation times (in seconds) on a simulation before and after the improvement with the matrix of signs. The results are presented after having simulated 1000 datasets of the standard Brownian motion observed in 101 equally spaced times of $[0; 1]$, the shift Δ is applied on the mean and $\Delta(t) = 2t$.

Method	[Minimum ; Maximum]	Mean (sd)
Basic method	[78 ; 120]	101 (8)
With the improvement	[0.25 ; 0.87]	0.34 (0.06)